

Signal-Mediated Depolymerization of Actin in Pollen during the Self-Incompatibility Response

Benjamin N. Snowman,^a David R. Kovar,^b Galina Shevchenko,^a Veronica E. Franklin-Tong,^{a,1} and Christopher J. Staiger^b

^a School of Biosciences, University of Birmingham, Edgbaston, Birmingham B15 2TT, United Kingdom

^b Department of Biological Sciences, Purdue University, West Lafayette, Indiana 47907-1392

Signal perception and the integration of signals into networks that effect cellular changes is essential for all cells. The self-incompatibility (SI) response in field poppy pollen triggers a Ca^{2+} -dependent signaling cascade that results in the inhibition of incompatible pollen. SI also stimulates dramatic alterations in the actin cytoskeleton. By measuring the amount of filamentous (F-) actin in pollen before and during the SI response, we demonstrate that SI stimulates a rapid and large reduction in F-actin level that is sustained for at least 1 h. This represents quantitative evidence for stimulus-mediated depolymerization of F-actin in plant cells by a defined biological stimulus. Surprisingly, there are remarkably few examples of sustained reductions in F-actin levels stimulated by a biologically relevant ligand. Actin depolymerization also was achieved in pollen by treatments that increase cytosolic free Ca^{2+} artificially, providing evidence that actin is a target for the Ca^{2+} signals triggered by the SI response. By determining the cellular concentrations and binding constants for native profilin from poppy pollen, we show that profilin has Ca^{2+} -dependent monomeric actin-sequestering activity. Although profilin is likely to contribute to stimulus-mediated actin depolymerization, our data suggest a role for additional actin binding proteins. We propose that Ca^{2+} -mediated depolymerization of F-actin may be a mechanism whereby SI-induced tip growth inhibition is achieved.

INTRODUCTION

The cytoskeleton is a major target for signaling cascades in animal and plant cells. In plant cells, light, touch, hormones, pathogen attack, and many other extracellular stimuli lead to rapid structural changes (Nick, 1999; Staiger, 2000). Many of the signaling intermediates that regulate actin dynamics are well defined in animal cells and yeast (for reviews, see Hall, 1998; Schmidt and Hall, 1998), but considerably less is known for plants. A major focus of plant cytoskeleton research is the identification of signals and signal transduction cascades that regulate actin dynamics (Staiger et al., 2000). Actin rearrangements in response to physiological cues have been described for responses of stomatal guard cells to abscisic acid or light, root hairs responding to Nod factors from *Rhizobium* bacteria, and pollen tubes responding to self-incompatibility (S) proteins (Eun and Lee, 1997; Cárdenas et al., 1998; de Ruijter et al., 1999; Miller et al., 1999; Geitmann et al., 2000). Although these articles describe structural filamentous (F-) actin reorganization and qualitative changes in phalloidin staining, they do not provide any quantitation of F-actin levels, which is necessary to demonstrate actin de-

polymerization. de Ruijter et al. (1999) quantified the fluorescence intensity of confocal microscopy images to ascertain the numbers of actin filament bundles in the tip region of bean root hairs. Although they report a local increase in fine actin bundles in response to lipochitooligosaccharides from *Rhizobium*, this is not the same as measuring polymerization levels. Thus, to date, no study on plants has characterized the effect that specific, physiologically relevant signaling stimuli have on the state of actin polymerization.

Tip-growing cells represent an ideal system in which to investigate the role of signal transduction in effecting changes to the actin cytoskeleton (Geitmann and Emons, 2000). In pollen tubes, the actin cytoskeleton plays an essential role during germination and tip growth, which involves targeted vesicle secretion (Gibbon et al., 1999; Vidali and Hepler, 2001). Other components that are thought to be necessary for normal pollen tube growth include a tip-based cytosolic free Ca^{2+} ($[\text{Ca}^{2+}]_i$) gradient, Ca^{2+} -dependent protein kinase, Rop GTPases, cAMP, actin organization, and F-actin levels (Estruch et al., 1994; Pierson et al., 1996; Messerli and Robinson, 1997; Gibbon et al., 1999; Fu and Yang, 2001; Moutinho et al., 2001; Vidali et al., 2001). However, cause-and-effect relationships between these components remain to be established.

Investigations into the signal-mediated inhibition of tip growth have been performed using pollen from the field

¹To whom correspondence should be addressed. E-mail v.e. franklin-tong@bham.ac.uk; fax 44-121-414-5925.

Article, publication date, and citation information can be found at www.plantcell.org/cgi/doi/10.1105/tpc.002998.

poppy undergoing the self-incompatibility (SI) response. SI involves highly specific “self”-recognition of pollen to prevent self-fertilization and consequent inbreeding. In poppy, SI is determined by a single, multiallele *S* gene (Lawrence et al., 1978). Allele-specific *S* proteins are secreted by the stigma and interact with pollen, resulting in the rapid inhibition of growth of “self” or incompatible, but not compatible, pollen. Stigmatic *S* alleles from poppy have been cloned, and the recombinant *S* proteins have *S*-specific inhibitory activity (Foote et al., 1994; Kurup et al., 1998). *S* proteins act as signal molecules, stimulating *S*-specific increases in $[Ca^{2+}]_i$ (Franklin-Tong et al., 1993, 1995, 1997, 2002). This is thought to trigger the Ca^{2+} -dependent hyperphosphorylation of a pollen protein, p26 (Rudd et al., 1996). Nuclear DNA fragmentation (Jordan et al., 2000) and evidence for a caspase-like activity (Rudd and Franklin-Tong, 2002) suggest that a programmed cell death signaling pathway is triggered by SI. More recently, we demonstrated that the SI response induces rapid alterations in actin cytoarchitecture in incompatible pollen tubes (Geitmann et al., 2000).

Here, we have investigated the SI-induced actin alterations further and provide quantitative evidence for the stimulus-mediated depolymerization of actin filaments in plant cells. Actin depolymerization also was achieved by treatments that increase $[Ca^{2+}]_i$ artificially. With evidence for Ca^{2+} -regulated actin binding proteins (ABPs) in pollen and measurement of their effects on actin *in vitro* (Gibbon and Staiger, 2000; Yokota and Shimmen, 2000), it is reasonable to assume that ABPs provide the link between stimulus and response. However, extremely few quantitative data regarding plant ABPs, such as cellular concentrations and equilibrium binding constants, are available at present. Attention is focused on profilin because it appears to be the major monomeric (G-) actin binding protein in pollen (Gibbon et al., 1999) and it has calcium-regulated actin-sequestering activity *in vitro* (Kovar et al., 2000a). We began to model the stimulus-mediated depolymerization during SI in poppy pollen through quantitative analyses of profilin and actin levels *in vivo* and measurements of native pollen profilin's sequestering activity *in vitro*. Our data implicate the involvement of other ABPs in addition to profilin. We discuss actin depolymerization as a mechanism for the inhibition of tip growth and propose that although the initial depolymerization may arrest growth, there could be additional roles for the sustained depolymerization in the SI response.

RESULTS

Dramatic Rearrangements of the Pollen Actin Cytoskeleton Are Stimulated during SI

Figure 1 shows representative images of pollen F-actin stained with fluorescent phalloidin. Figures 1A to 1C provide reference points for both the quantitation and imaging of

F-actin in pollen grains (see below); similar images have been published previously (Geitmann et al., 2000). In normally growing pollen tubes, thick actin bundles were detected in the shank region, with a “basket-like” structure of fine F-actin bundles located ~5 to 10 μ m from the apex, and a zone of less intense phalloidin staining at the tip (Figure 1A). When SI was induced in pollen tubes, within 5 min many F-actin bundles were lost and the overall intensity of phalloidin staining was reduced substantially, although cortical F-actin was retained (Figure 1B). At later time points, punctate foci of actin were observed (Figure 1C). These changes were not detected in pollen tubes treated with compatible *S* proteins (data not shown).

Because the SI response of poppy *in vivo* typically occurs before, or soon after, pollen germination on the stigma, we also performed SI inductions on pollen grains (Figures 1D to 1I). In untreated, hydrated pollen grains (Figures 1D and 1E), F-actin bundles were highly organized in a “cage” around the generative cell and vegetative nucleus. Cytoplasmic and cortical F-actin also were quite prominent. SI induction in pollen grains gave a similar, but slower, actin response than that seen in pollen tubes. At 20 min after the addition of incompatible *S* proteins (Figures 1F and 1G), many of the cytoplasmic actin filaments were lost, whereas F-actin adjacent to the plasma membrane was more prominent (Figure 1G), suggesting that it was either retained or increased. For comparison, we also examined control pollen grains 20 min after the addition of germination medium (GM; Figure 1H). Germination had occurred already, and the characteristic organization of F-actin in the tip region was observed. The localization of F-actin clearly contrasts with that seen in an incompatible pollen grain at a comparable time point. The F-actin cage around the generative cell and the vegetative nucleus was no longer apparent (Figure 1H), and there were abundant F-actin bundles throughout the cytosol. During the later stages of SI in pollen grains, punctate foci of actin also were detected (Figure 1I). These observations clearly demonstrate that very similar alterations to the actin cytoskeleton occur in pollen grains during the SI response and strongly suggest that F-actin depolymerization might be responsible for some of the SI-induced alterations.

Quantitative Analysis of F-Actin Levels in Pollen Grains and Tubes

To investigate whether F-actin depolymerization was triggered by the SI response in pollen, we determined the amount of polymeric actin in poppy pollen using a biochemical method to quantify fluorescent phalloidin binding (Howard and Oresajo, 1985b; Lillie and Brown, 1994; Yeh and Haarer, 1996) that has been adapted for use in plant cells (Gibbon et al., 1999). Polymer levels in pollen during hydration, germination, and tube growth were measured (Figure 2A). Hydrated pollen grains ($t = 1$ min) had a mean concentration of actin in the polymeric form of $14.7 \pm 3.3 \mu$ M (mean \pm SE; $n = 10$). The level of polymeric actin in pol-

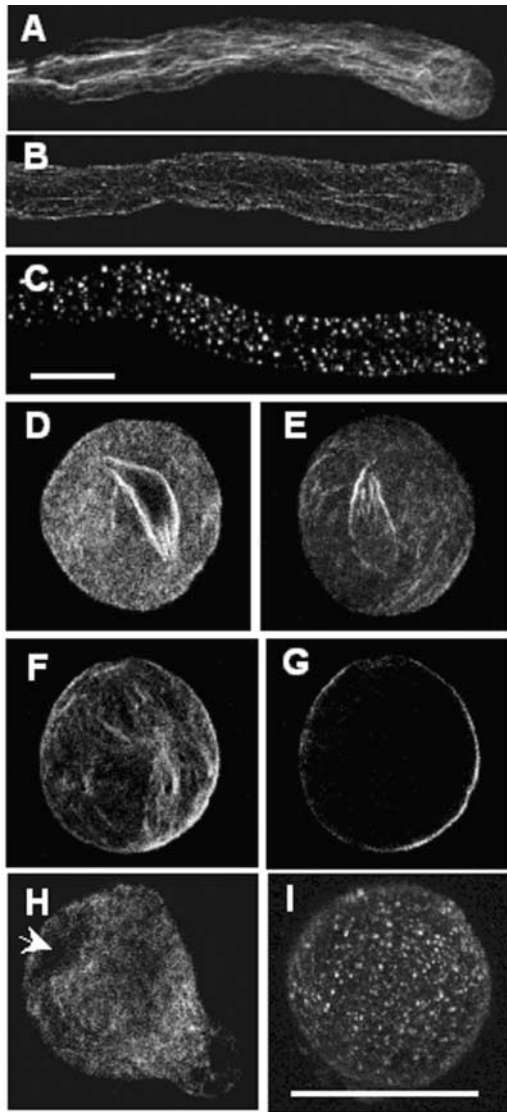


Figure 1. Rearrangements of the Pollen F-Actin Cytoskeleton Are Triggered by SI.

Alexa-488-phalloidin-stained pollen grains and tubes of poppy were imaged using confocal microscopy. (A) to (D), (F), and (I) show z-series projections through half of the pollen tube or pollen grain. (E), (G), and (H) show single optical sections from a medial plane. Bar in (C) = 10 μ m for (A) to (C); bar in (I) = 25 μ m for (D) to (I).

(A) Growing pollen tube with a normal F-actin configuration.

(B) Typical F-actin configuration in an incompatible pollen tube at 5 min after SI induction. Cytoplasmic F-actin appears reduced and fragmented; cortical actin is unaffected.

(C) Incompatible pollen tube at 60 min after SI has numerous punctate foci of F-actin.

(D) Typical F-actin configuration in an untreated pollen grain. A cage-like F-actin structure lies around the generative cell and the vegetative nucleus.

(E) Optical section midway through an untreated grain. Cytoplasmic F-actin is prominent, as is the cage-like F-actin structure. Although cortical actin is present, it is not prominent.

len tubes grown on GM for 60 min was $16.1 \pm 2.1 \mu\text{M}$ ($n = 12$). Comparisons between the levels of F-actin measured in pollen grains or tubes that had been in contact with GM between 1 and 120 min showed no significant changes ($P = 0.5$ by analysis of variance [ANOVA]) in F-actin in pollen grains or tubes during this period.

To demonstrate that reductions in F-actin levels could be measured, poppy pollen tubes were treated with latrunculin B (LatB), a potent actin-depolymerizing agent (Gibbon et al., 1999). Pollen tubes that had been grown for 50 min were challenged for 10 min with 100 nM, 1 μM , and 10 μM LatB. This treatment resulted in F-actin levels of $6.6 \pm 0.6 \mu\text{M}$ ($n = 4$), $4.5 \pm 0.5 \mu\text{M}$ ($n = 4$), and $1.1 \pm 0.3 \mu\text{M}$ ($n = 4$), respectively. F-actin levels in all LatB-treated tubes were significantly different ($P < 0.03$) from those of a control incubated in GM with 0.5% DMSO, which had an F-actin level of $10.2 \pm 1.1 \mu\text{M}$ ($n = 4$). This finding demonstrated that the phalloidin binding assay was appropriate to measure rapid changes in F-actin levels in poppy pollen.

The SI Response Involves F-Actin Depolymerization

Having established that we could measure F-actin depolymerization, we investigated whether the SI response stimulated alterations to F-actin levels in pollen tubes. An incompatible SI challenge resulted in a marked reduction of F-actin levels in pollen tubes, as shown in Figure 2B. At 1 min after SI induction, F-actin levels had decreased to $9.9 \pm 1.7 \mu\text{M}$ ($n = 6$). Controls, which involved additions of GM and incompatible heat-denatured S proteins for 1 min, gave F-actin levels of $14.9 \pm 2.8 \mu\text{M}$ ($n = 6$) and $16.1 \pm 3.8 \mu\text{M}$ ($n = 4$), respectively. By 5 and 10 min after SI challenge, F-actin levels had decreased to $6.8 \pm 2.0 \mu\text{M}$ ($n = 6$) and $5.0 \pm 1.4 \mu\text{M}$ ($n = 6$), respectively. By 60 min after challenge, the F-actin level was $3.0 \pm 0.6 \mu\text{M}$ ($n = 6$). This finding clearly demonstrates rapid F-actin depolymerization. Compatible pollen treated with the same S proteins for 20 min did not show changes in F-actin levels ($15.2 \mu\text{M}$; $n = 2$). Pollen tubes treated for 60 min with either incompatible

(F) F-actin in a pollen grain at 20 min after SI. No nuclear actin cage is seen, but some F-actin bundles are evident.

(G) Optical section midway through the SI grain in (F) reveals the virtually complete loss of cytoplasmic F-actin, but cortical F-actin is retained or increased.

(H) Optical section showing F-actin configuration in a control pollen grain at 20 min. Germination has occurred; note the typical F-actin arrangement in the pollen tube tip region. Cytoplasmic F-actin is present, but the nuclear actin cage is less evident; the generative cell and the vegetative nucleus are located away from the tip (arrow). In contrast to (G), there are abundant F-actin bundles throughout the cytosol.

(I) Pollen grain at 60 min after SI showing numerous punctate F-actin foci.

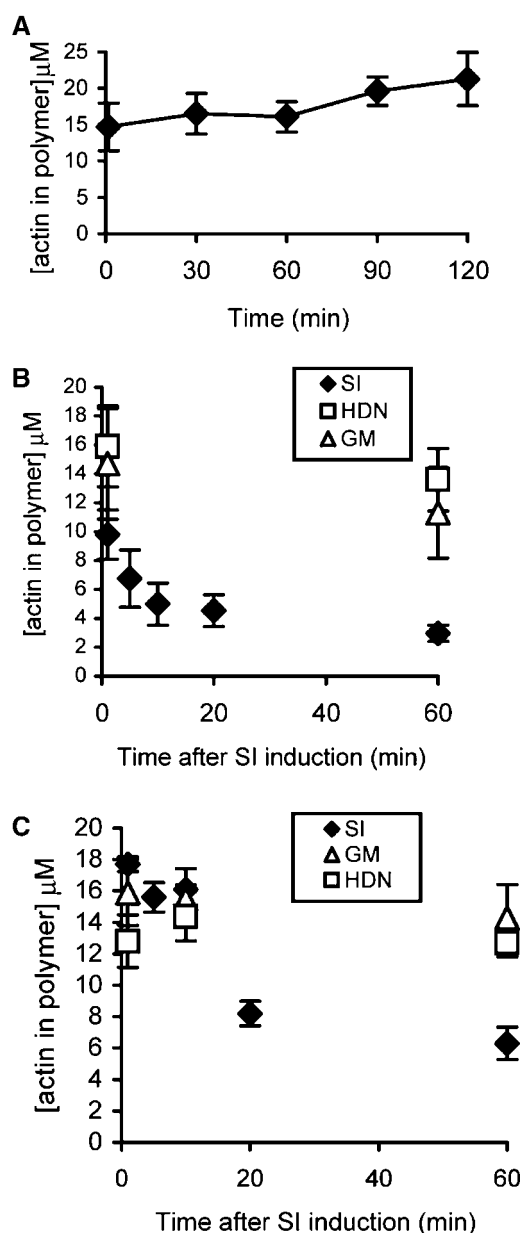


Figure 2. The SI Response Induces F-Actin Depolymerization.

The concentration of actin in the polymerized form in pollen grains and tubes was measured using the Alexa-488–phalloidin binding assay.

(A) Pollen was grown in vitro for the times indicated and the amounts of actin in polymeric form were measured. Mean values \pm SE ($n = 8$ to 25) are plotted.

(B) F-actin levels in pollen tubes during SI. Pollen was grown for 60 min (equivalent to time 0), treated with incompatible S proteins (closed diamonds), and samples were collected at time intervals after SI induction. Controls were treated in the same way with heat-denatured (HDN) –incompatible S proteins (open squares) or GM (open triangles). Each data point represents mean values \pm SE ($n = 6$), except for HDN controls ($n = 4$).

heat-denatured S proteins or GM gave F-actin values of $13.7 \pm 3.1 \mu\text{M}$ ($n = 4$) and $11.4 \pm 2.2 \mu\text{M}$ ($n = 6$), respectively. These values were similar to the levels found in untreated pollen tubes and were significantly different from those for 60-min SI treatments ($P < 0.004$). The percentage of F-actin reduction as a consequence of SI challenge was 74%, compared with the GM control at 60 min. Therefore, our data clearly demonstrate that the SI response triggers rapid and massive F-actin depolymerization that is sustained for a considerable period of time.

Although SI can be stimulated in pollen tubes in vitro, under in vivo conditions, it normally occurs in pollen grains before or soon after polarity is established. Therefore, we wished to determine if F-actin depolymerization also occurred in pollen grains. Reductions in F-actin levels in pollen grains, compared with the response in pollen tubes, were somewhat delayed (Figure 2C). F-actin levels at 1 and 10 min after SI challenge were $17.7 \pm 0.5 \mu\text{M}$ ($n = 4$) and $16.1 \pm 1.3 \mu\text{M}$ ($n = 4$), which were not significantly different ($P > 0.4$) from those of the GM controls at the same time points. However, at 20 min after SI induction, F-actin levels were reduced to $8.2 \pm 0.8 \mu\text{M}$ ($n = 4$), and they were reduced further to a mean of $6.3 \pm 1.0 \mu\text{M}$ ($n = 4$) at 60 min. This value was significantly different from that of the GM control at this time point ($14.4 \pm 2.1 \mu\text{M}$) and represents a 56% reduction in F-actin levels. This finding clearly demonstrates that F-actin depolymerization is stimulated in pollen grains during the SI response.

Cessation of Tip Growth Does Not Reduce F-Actin Levels

Because SI inhibits tip growth, we wished to establish whether the F-actin depolymerization observed was a consequence of growth inhibition or whether it was attributable specifically to the SI signaling cascade. We used caffeine, which inhibits tip growth by dissipating the tip-localized $[\text{Ca}^{2+}]_i$ gradient (Pierson et al., 1996). Poppy pollen growth is inhibited by 10 mM caffeine, and only slight changes to the F-actin cytoarchitecture were detected after 10 min (Geitmann et al., 2000). Caffeine had no effect on F-actin levels; pollen tubes treated for 20 min had $17.8 \pm 1.0 \mu\text{M}$ ($n = 4$) actin in the polymeric form, compared with $17.0 \pm 0.4 \mu\text{M}$ ($n = 4$) for tubes treated with GM in the same experiment ($P = 0.5$). Therefore, our data suggest that the SI response signals depolymerization of F-actin specifically, rather than a nonspecific response as a result of growth cessation.

(C) F-actin levels in pollen grains during SI. Pollen was sown directly onto GM-containing incompatible S proteins (closed diamonds), HDN-incompatible S proteins (open squares), or GM (open triangles).

Increases in Cytosolic Calcium Result in Changes in F-Actin

Increases in $[Ca^{2+}]_i$ in poppy pollen tubes are triggered during the SI response, and $[Ca^{2+}]_i$ is thought to act as a second messenger for the SI-specific signal transduction cascade. To determine whether F-actin is a target for a Ca^{2+} -dependent signaling cascade, we used two treatments known to induce increases in $[Ca^{2+}]_i$, the Ca^{2+} ionophore A23187 and mastoparan (Franklin-Tong et al., 1996), to determine whether artificial increases in $[Ca^{2+}]_i$ also triggered a reduction in F-actin levels. Because pollen grains are difficult to microinject, nothing is known about $[Ca^{2+}]_i$ in pollen grains, although it is anticipated to be similar. Therefore, we confined our studies to pollen tubes.

The addition of 50 μ M A23187 stimulated F-actin depolymerization (Figure 3A), with a decrease from $10.0 \pm 0.9 \mu$ M ($n = 3$) at 1 min to $3.6 \pm 0.4 \mu$ M ($n = 3$) at 30 min. The 30-min value represented a 59% depolymerization of F-actin relative to the GM control at the same time point, and this level of depolymerization was sustained, because no further significant alterations were detected during the subsequent 90 min ($P = 0.24$). Treatment of pollen tubes with 25 μ M mastoparan also stimulated F-actin depolymerization (Figure 3B), with F-actin levels reduced to $5.1 \pm 0.3 \mu$ M ($n = 9$) after 5 min. Compared with controls treated with GM for 20 min, this constituted a decrease of 51%, and no significant additional decreases were seen during the 20-min period investigated ($P = 0.8$ by ANOVA).

We also investigated the F-actin configuration during responses of poppy pollen tubes to treatment with A23187 (Figures 4A to 4D) and mastoparan (Figures 4E and 4F). A23187 had several effects on the F-actin cytoarchitecture. By 30 min, 32.4% of pollen tubes had small punctate foci of F-actin (Figure 4A), and 38.5% had F-actin that appeared fragmented and bundled (Figure 4B). A high proportion of the F-actin bundles were distributed adjacent to the plasma membrane (Figure 4C). As observed previously (Geitmann et al., 2000), 18.7% of pollen tubes showed normal F-actin organization, and 8.8% could not be classified. By 120 min, pollen tubes treated with A23187 had large punctate aggregates or foci of F-actin (Figure 4D). Treatment with mastoparan resulted in a reduction in phalloidin staining in the apical region and the formation of small punctate foci of F-actin (Figures 4E and 4F). This response was rapid, because there were no apparent differences between cells treated for 5 and 20 min. Together, our data suggest that considerable changes are induced in the F-actin cytoskeleton in response to increases in $[Ca^{2+}]_i$ and that these changes involve actin depolymerization.

Viability of Pollen during Actin Depolymerization

Viability data relating to the early phase of the SI response are provided in Figure 5. Fluorescein diacetate, an estab-

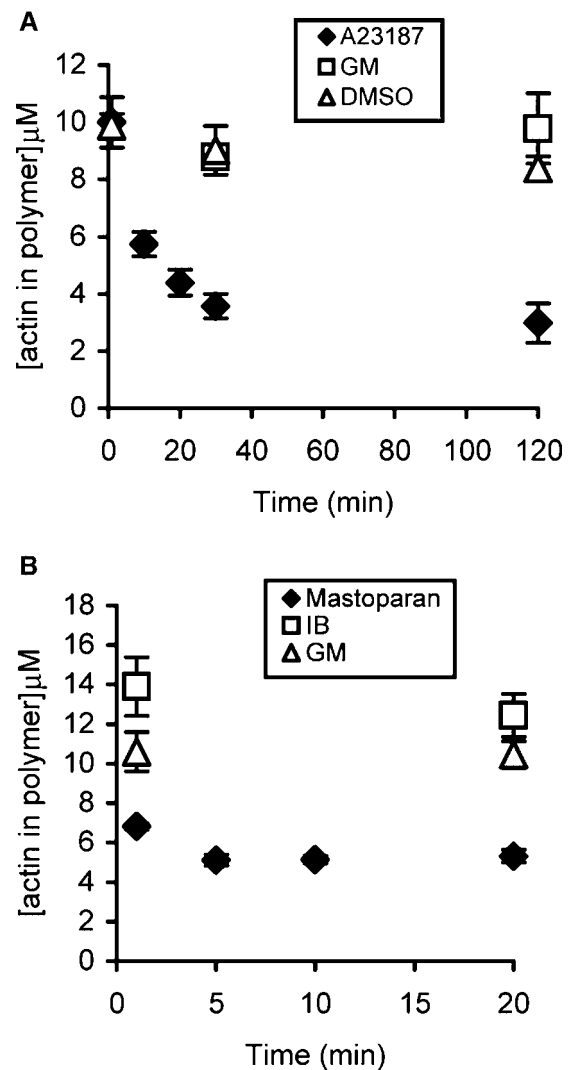


Figure 3. Drugs That Increase $[Ca^{2+}]_i$ Result in Depolymerization of F-Actin.

Pollen tubes were treated with drugs known to increase $[Ca^{2+}]_i$ in poppy pollen tubes, and the concentration of actin in polymeric form was measured.

(A) A23187 (50 μ M; closed diamonds) stimulated F-actin depolymerization. Controls were GM (open squares) and 0.5% DMSO in GM (open triangles). Each data point represents mean values \pm SE ($n \geq 3$).

(B) Mastoparan (25 μ M; closed diamonds) reduced F-actin levels. Each data point represents mean values \pm SE ($n \geq 6$). Controls were injection buffer (IB; open squares) and GM (open triangles).

lished marker for cell viability that has been used for pollen, was used in our experiments. We collected data to ascertain viability during the first 20 min of the SI response in pollen tubes, because this is when the dramatic actin depolymerization phase occurs. Our data indicate no significant

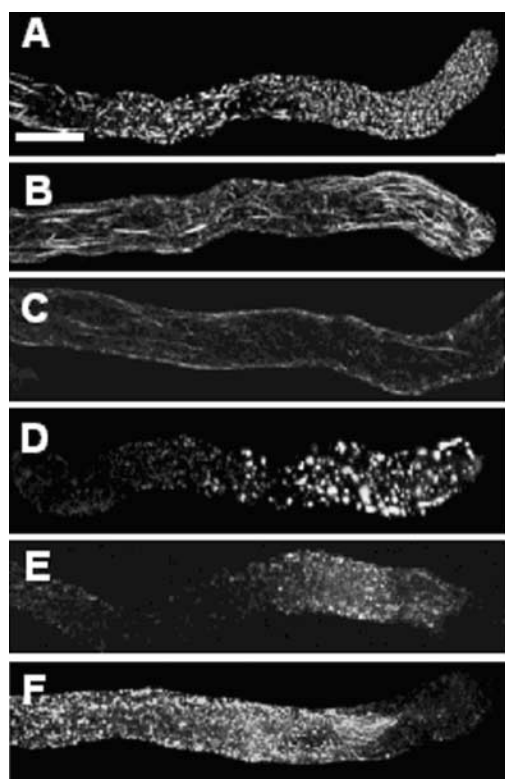


Figure 4. Actin Organization Is Perturbed by Ca^{2+} Agonists.

Pollen tubes were treated with drugs known to increase $[\text{Ca}^{2+}]_i$ in poppy pollen tubes, and the F-actin cytoskeleton was imaged using fluorescent phalloidin. All images, except (D), show z-series projections that reconstruct half a pollen tube. Bar in (A) = 10 μm .

(A) to (D) Treatment with 50 μM A23187.

(A) At 30 min, long F-actin bundles were lost and small punctate foci of F-actin formed.

(B) At 30 min, F-actin appeared as fragmented bundles, often with a fan-like configuration at the apex.

(C) An optical section shows F-actin adjacent to the plasma membrane.

(D) After 120 min, F-actin formed larger punctate foci.

(E) and (F) Treatment with 25 μM mastoparan.

(E) At 5 min, long F-actin bundles were lost, the apical region was virtually free of F-actin, and punctate foci of F-actin were detectable.

(F) Treatment for 20 min resulted in no further changes.

difference in viability at 0, 10, and 20 min ($P = 0.089$ by ANOVA). We also collected data for 40- and 60-min time points, when the F-actin concentration was no longer decreasing. Although there was no significant difference in viability at 0, 10, 20, and 40 min ($P = 0.154$ by ANOVA), there was a highly significant reduction in viability at 60 min ($P < 0.001$ by ANOVA). We also obtained preliminary data using Mitotracker Red CMXRos, which accumulates only in functional, active mitochondria (data not shown); these data in-

dicated that a significant number of pollen tubes were still viable during this time period. A previous study of viability at later time points indicates that cells die at ~ 4 h after the SI response (Jordan et al., 2000).

Total Actin and Profilin Concentrations in Pollen

Cellular changes in actin organization and dynamics are thought to be regulated by ABPs. In pollen, the best-characterized ABPs are profilin, ADF/cofilin, and 135-ABP (villin-like) (Gibbon and Staiger, 2000; Kovar and Staiger, 2000; Yokota and Shimmen, 2000), although there is circumstantial evidence for several others. Given the presumed role of pollen profilin as a monomeric actin-sequestering factor and the recent demonstration of its regulation by calcium (Kovar et al., 2000a), this protein seemed a logical candidate to transduce the increases in $[\text{Ca}^{2+}]_i$ during SI into F-actin depolymerization. To calculate whether profilin can account for F-actin depolymerization at different Ca^{2+} concentrations, it was necessary to measure the cellular concentrations of the relevant proteins and to determine equilibrium binding constants under physiologically relevant conditions *in vitro*.

The cellular concentrations of pollen profilin and the total actin pool were determined by ELISA (Gibbon et al., 1999). To confirm the specificity of antisera on pollen extracts, SDS-PAGE and protein gel blot analyses were performed. Profilin and actin antisera cross-reacted specifically with the appropriate proteins from poppy pollen extracts and with purified native proteins (Figure 6). We performed ELISAs using these antisera to determine the amount of profilin and total actin in poppy pollen (Table 1). Control pollen grains and tubes had profilin and actin present in approximately a 1:1 stoichiometry, as was observed previously for maize (Gibbon et al., 1999) and lily pollen (Vidali and Hepler, 1997). In hydrated ungerminated grains, the total actin concentration was 299 μM , and that of profilin was 234 μM . Pollen tubes treated with GM for 1 min contained 247 μM total actin and 195 μM profilin. As a percentage of total protein, profilin was $0.6 \pm 0.1\%$ ($n = 4$) in both pollen tubes and pollen grains. Total actin was $2.4 \pm 0.1\%$ ($n = 4$) in pollen tubes and $2.2 \pm 0.5\%$ ($n = 4$) in pollen grains.

During the SI response, actin and profilin levels remained stable in pollen grains (Table 1). After 60 min of SI, the total actin concentration was 305 μM , and that of profilin was 234 μM . These values were not significantly different from those of grains treated with GM for 60 min ($P > 0.3$) or grains treated with S protein for 1 min ($P > 0.3$). Pollen tubes showed modest reductions in both actin and profilin levels after challenge with S protein. The total actin concentration was 201 μM , and that of profilin was 156 μM after 60 min. The actin concentration was not significantly different from that observed in pollen tubes treated for 1 min with S protein ($P = 0.46$), but it was different from that found with the 60-min GM treatment ($P = 0.006$). Profilin concentration in 60-min SI tubes was not significantly different from that of

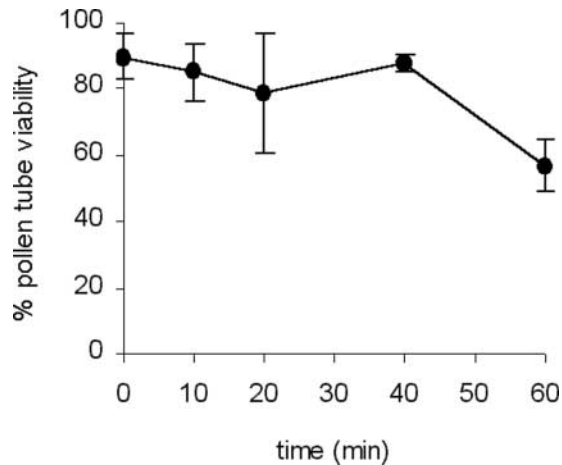


Figure 5. Viability of Pollen Is Retained during the Actin Depolymerization Process.

The plot shows the percentage of pollen viability, as measured by fluorescein diacetate staining at 0, 10, 20, 40, and 60 min after treatment with incompatible S proteins. The mean percentage of pollen that stained with fluorescein diacetate (\pm SD) was 89.6 ± 6.9 ($n = 14$), 84.9 ± 8.8 ($n = 10$), 78.8 ± 17.9 ($n = 10$), 87.7 ± 2.5 ($n = 3$), and 56.9 ± 7.9 ($n = 7$) for these time points, respectively. There was no significant difference in the viability of pollen tubes between 0 and 40 min after SI induction. However, by 60 min, viability was reduced significantly.

1-min SI tubes ($P = 0.1$), but it was different from that of the 60-min GM control ($P = 0.02$). The latter may reflect sampling error, because profilin as a percentage of total protein did not change during this time course (data not shown).

Calcium Stimulates Profilin-Sequestering Activity

To determine whether profilin can account for the size of the F-actin pool in unstimulated pollen and whether it is capable of reducing the level of actin filaments in the presence of increased calcium, we reconstituted the situation in vitro using purified native poppy pollen profilin and native maize pollen actin. Apparent K_d values for profilin binding to actin and the prevention of polymerization were measured at steady state, in the presence of uncapped filament ends, with a light-scattering assay described previously (Kovar et al., 2000a). As was found for maize pollen profilin, when free Ca^{2+} concentration was increased, the amount of actin polymerization decreased in the presence of native poppy profilin. At 200 nM Ca^{2+} , which is comparable to what might be found in the shank of the pollen tube during normal growth (Rathore et al., 1991; Miller et al., 1992; Pierson et al., 1996), the apparent K_d was $2.2 \pm 0.7 \mu\text{M}$ ($n = 3$) (Table 2). At 2 μM Ca^{2+} , a concentration similar to the pulses of cytosolic calcium at the tip of actively growing tubes (Holdaway-Clarke

et al., 1997; Messerli and Robinson, 1997) and to the Ca^{2+} wave during SI (Franklin-Tong et al., 1997), the apparent K_d was $1.2 \pm 0.3 \mu\text{M}$ ($n = 3$). This twofold difference in apparent sequestering activity is somewhat lower than that reported for native maize pollen profilin at high and low Ca^{2+} concentrations (Kovar et al., 2000a).

Role of Ca^{2+} in Actin Depolymerization—A Simulation

Through detailed understanding of the activity of pollen ABPs, a model of how F-actin levels are reduced in response to SI can be formulated. If we model the interaction of poppy profilin with actin at steady state using the equations and assumptions of Gibbon et al. (1999) and the data obtained here, we can assess whether there is enough profilin present to account for the actin depolymerization observed during SI. For 200 nM Ca^{2+} (basal $[\text{Ca}^{2+}]_i$ in pollen tubes) (Rathore et al., 1991; Miller et al., 1992; Pierson et al., 1996; Franklin-Tong et al., 1997), using the total actin concentration of 221 μM , the total profilin concentration of 194 μM , a critical concentration for actin of 0.4 μM , and the apparent K_d value of 2.2 μM , the concentration of actin present in the polymeric form is predicted to be 37.3 μM . This value is twofold to threefold greater than what was measured here for poppy pollen and previously for maize pollen (Gibbon et al., 1999). When Ca^{2+} levels are 10-fold higher, as they are during SI (Franklin-Tong et al., 1997), the critical concentration for actin is 0.48 μM , and the apparent K_d value for profilin actin is 1.2 μM . Because we have shown that profilin and total actin levels do not change markedly during the initial SI response, the amount of actin in the polymeric form at 2 μM Ca^{2+} is predicted to be 33.5 μM . Thus, a 10% reduction in F-actin levels caused by enhanced profilin-sequestering activity is predicted by this model. Even if basal Ca^{2+} levels were 100 nM in the pollen tube, with an apparent K_d value for profilin binding to actin of 2.8 μM , the predicted change in F-actin levels caused by profilin would be only 16%. This is very different from the 56 to 74% depolymerization observed.

DISCUSSION

We have measured a rapid, considerable, and sustained F-actin depolymerization stimulated by the SI response. Our data are significant for two reasons. First, this study provides quantitative measurements of alterations to F-actin levels in a plant cell by a defined biological stimulus. Second, we have measured an unequivocal depolymerization, and there are remarkably few examples of this stimulated by a biologically relevant ligand. Quantification of F-actin levels was achieved by adapting a powerful assay that reports the number of fluorescent-phalloidin binding sites in a cell (Howard and Oresajo, 1985b; Lillie and Brown, 1994;

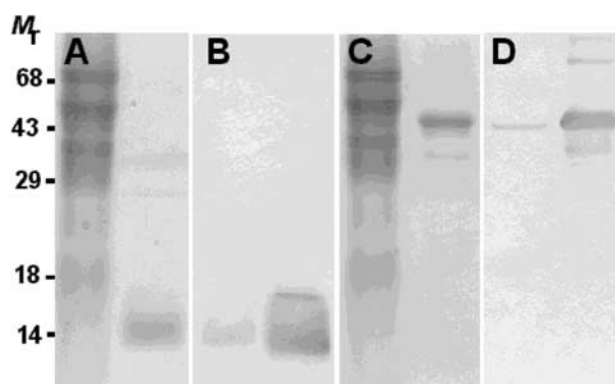


Figure 6. Profilin and Actin Antisera Recognize Poppy Proteins Specifically.

Polyclonal antisera raised against maize pollen actin and profilin were tested against pollen extracts. Also shown is the purity of the purified actin and profilin from poppy pollen used as standards for ELISA. The migration of molecular mass standards is shown at left.

(A) Coomassie blue-stained SDS gel loaded with 50 μ g of poppy pollen cytosolic extract (lane 1) and 1 μ g of purified poppy pollen profilin (lane 2).

(B) A gel identical to that shown in **(A)** was blotted and probed with anti-ZmPRO3, which cross-reacted with a single, 14-kD polypeptide in pollen cytosol (lane 1) and with purified poppy pollen profilin (lane 2).

(C) Coomassie blue-stained SDS gel loaded with 50 μ g of poppy pollen cytosolic extract (lane 1) and 1 μ g of purified poppy pollen actin (lane 2).

(D) A gel identical to that shown in **(C)** was blotted and probed with anti-maize pollen actin serum, which cross-reacted with a single polypeptide of 42 kD in the pollen cytosol (lane 1) and with purified poppy pollen actin (lane 2).

Gibbon et al., 1999). Although several studies have described changes to the plant actin cytoskeleton in response to physiological stimuli (Eun and Lee, 1997; Kobayashi et al., 1997; Cárdenas et al., 1998; de Ruijter et al., 1999; Miller et al., 1999), they all used F-actin imaging without quantitative analysis. Therefore, it is not possible to determine whether these alterations involve reorganization or changes in the polymerization status of actin. These quantitative data, together with those obtained from maize pollen (Gibbon et al., 1999), are the only such measurements that exist for plant cells.

F-Actin Depolymerization Is Sustained during SI

The pollen SI actin response differs significantly from that found in most other studies that measure alterations in actin polymerization levels. In most signaling responses for which accurate measurements exist, extracellular stimuli lead to the polymerization of actin (Carlsson et al., 1979; Howard

and Oresajo, 1985a; Hall et al., 1988; Greenberg et al., 1991; Downey et al., 1992; Becker and Hart, 1999). However, some examples of rapid actin depolymerization exist (Ding et al., 1991; Lillie and Brown, 1994; Yeh and Haarer, 1996; Aizawa et al., 2001). For example, during the heat shock response of yeast, a 25 to 50% reduction in F-actin is observed within 30 s, but levels return to normal within 3 min (Lillie and Brown, 1994). Although the actin depolymerization measured during SI was equally rapid, it led to an even greater loss of actin filaments, and depolymerization was sustained for at least 1 h.

F-actin depolymerization over several hours has been identified as a feature of apoptosis (Levee et al., 1996; Janmey, 1998; Korichneva and Hämmerling, 1999; Rao et al., 1999). Because there is evidence that a programmed cell death signaling cascade is stimulated in the SI response (Jordan et al., 2000; Rudd and Franklin-Tong, 2002), this might indicate a potential reason why actin depolymerization is more sustained than expected. In some cell types, actin is a target for caspase activity (Janmey, 1998). Although there are no caspase orthologs in the Arabidopsis genome, a number of studies indicate that caspase-like activities are triggered by programmed cell death in plant cells (del Pozo and Lam, 1998; D'Silva et al., 1998; Korthout et al., 2000; Richael et al., 2001). Indeed, there is preliminary evidence for caspase-like activity stimulated during SI (N.D. Jordan and V.E. Franklin-Tong, unpublished data). A link between a programmed cell death signaling cascade and the sustained depolymerization of F-actin should be explored in future studies.

Role of Ca^{2+} and Actin Binding Proteins in Actin Depolymerization

We demonstrated previously that the SI response triggers rapid and large increases in $[\text{Ca}^{2+}]_i$ (Franklin-Tong et al., 1993, 1995, 1997, 2002). Here, we have shown that artificially increasing $[\text{Ca}^{2+}]_i$ stimulates actin remodeling and a large decrease in F-actin in pollen. This finding suggests that the SI-induced Ca^{2+} increases target the actin cytoskeleton and that this results in actin depolymerization. Although two early studies show that increasing $[\text{Ca}^{2+}]_i$ artificially can disrupt actin filaments in pollen tubes (Kohno and Shimmen, 1987, 1988), no evidence to support the proposal that severing activity is activated was presented. In the present study, we conclude that the increases in $[\text{Ca}^{2+}]_i$ stimulated by SI are responsible for reducing actin polymer levels.

The critical concentration for pollen actin assembly does not change substantially over the 10-fold range of Ca^{2+} concentrations tested (Kovar et al., 2000a). This fact suggests that the reduction in F-actin is mediated through the action of specific ABPs. Depolymerization of actin filaments could result from a reduction in cross-linking or bundling activities, capping of filament ends, increased severing, inhibition of

Table 1. Quantitative Analysis of Total Actin and Profilin in Pollen

	Controls		SI Induced	
	[Profilin] (μM)	[Total Actin] (μM)	[Profilin] (μM)	[Total Actin] (μM)
Grains				
1 min	234 \pm 34	299 \pm 47	228 \pm 9	274 \pm 18
60 min	225 \pm 24	336 \pm 19	234 \pm 13	305 \pm 20
Tubes				
1 min	195 \pm 36	247 \pm 15	194 \pm 8	221 \pm 24
60 min	225 \pm 12	369 \pm 40	156 \pm 19	201 \pm 9

Controls were treated with GM for the times indicated and were tested in parallel with the SI treatments. All values are mean \pm SE ($n = 4$).

nucleation, or increases in monomer sequestering (Karpova et al., 1995; Cooper and Schafer, 2000). However, very few plant studies have attempted to reconstitute actin-ABP interactions under physiological conditions or to measure the cellular concentrations of protein or equilibrium binding constants between partners, so these ABP activities remain largely speculative. Many eukaryotic ABPs with these activities are regulated by Ca^{2+} (Kreis and Vale, 1999), but few have been identified and characterized in pollen tubes (Hepler et al., 2001; McCurdy et al., 2001).

ADF/cofilin proteins can cause the depolymerization of actin filaments and are regulated by Ca^{2+} indirectly via a Ca^{2+} -dependent protein kinase (Bamburg, 1999). When maize ADF is phosphorylated, its actin binding activity is inhibited (Smertenko et al., 1998; Allwood et al., 2001). Because increases in $[\text{Ca}^{2+}]_i$ are expected to prevent actin filament depolymerization through ADF, ADF/cofilin is an unlikely candidate for mediating the SI-induced actin depolymerization. 135-ABP is a villin-like protein from lily pollen that has Ca^{2+} /calmodulin-regulated actin-bundling activity (Yokota et al., 2000). However, 135-ABP has never been demonstrated to cap, sever, or depolymerize actin filaments. Nevertheless, bundling proteins can stabilize actin filaments in yeast (Karpova et al., 1995) and plant cells (Kovar et al., 2000b). At high $[\text{Ca}^{2+}]_i$, the release of 135-ABP from actin filaments could result in filament destabilization. Unfortunately, the lack of data regarding the cellular concentrations of 135-ABP in pollen or measurements of its affinity for F-actin make modeling its potential function during SI impractical at present.

Profilin is an abundant protein that either sequesters monomeric actin or shuttles actin onto filament barbed ends (Kang et al., 1999). The exact role of profilin in regulating actin polymerization depends on the cell type, the ratio of profilin to total actin, and the presence of other ABPs (Schlüter et al., 1997; Gibbon and Staiger, 2000). We recently demonstrated that physiologically relevant changes in Ca^{2+} can have marked effects on the sequestering activity of pollen

profilins (Kovar et al., 2000a). In maize and lily pollen, profilin is approximately equimolar with the total actin pool (Vidali and Hepler, 1997; Gibbon et al., 1999), and the apparent binding constant of maize profilin for maize pollen actin is high enough to account for the observation that only $\sim 10\%$ of the total actin is present in the polymeric form (Gibbon et al., 1999; Kovar et al., 2000a). Our prediction is that the bulk of unpolymerized actin in pollen is bound to profilin, which agrees with what has been measured in *Acanthamoeba* cells (Kaiser et al., 1999). Thus, a model in which profilin acts as a buffer for the G-actin pool and is the major ABP responsible for maintaining low levels of polymeric actin in pollen seems justifiable. However, we cannot exclude the possibility that an indirect effect of Ca^{2+} signaling (e.g., Ca^{2+} -dependent phosphorylation) also might modify profilin or profilin-interacting proteins.

In poppy pollen, profilin also is equimolar with the total actin pool, and its apparent K_d for actin is sufficient to account for the small size of the F-actin pool. Unlike the situation for native maize pollen profilin, in which an increase to micromolar Ca^{2+} concentrations shifts the apparent K_d 3.6-fold (Kovar et al., 2000a), for poppy profilin, a 2-fold change was observed. This finding indicates that increased sequestering activity will account for only a 10 to 16% reduction in polymer levels. Therefore, profilin on its own cannot account for the 56 to 74% reduction in F-actin levels during SI. However, our in vitro assays were performed in the presence of uncapped filament ends, and we assume no profilin-actin addition to barbed ends (Kovar et al., 2000a). Profilin behavior depends on the availability of barbed filament ends (Kang et al., 1999), and Ca^{2+} -loaded actin, when bound to profilin, does not add to filament ends (Gutsche-Perelroizen et al., 1999). Changes in Ca^{2+} concentration not only could regulate profilin and profilin/actin activity but also could modulate the state of filament ends. Although no bona fide capping factor has been identified from plants at present, the Arabidopsis genome (Arabidopsis Genome Initiative, 2000) contains heterodimeric CP- and CAPG-like genes.

Table 2. Apparent K_d Values for Poppy Profilin Binding to Pollen G-Actin at Different Calcium Concentrations

[Calcium] (nM)	K_d	n
100 ^a	2.8 \pm 0.4	4
200	2.2 \pm 0.7	3
1000	1.3 \pm 0.2	4
2000	1.2 \pm 0.3	3

The apparent K_d (μM ; mean \pm SD) values for binding to pollen G-actin under various physiological concentrations of Ca^{2+} were determined by measuring the shift in critical concentration at steady state.

^aThe K_d value at 100 nM Ca^{2+} was significantly different from the K_d values at both 1 μM and 2 μM by the two-tailed t test ($P < 0.003$).

One possible explanation for depolymerization during SI is that Ca^{2+} also activates a capping factor. This would result in profilin acting as a simple sequestering protein (Kang et al., 1999) and theoretically would allow even greater actin depolymerization.

Another possibility is that Ca^{2+} regulates a coordinated response of several different ABPs, including a side binding/bundling protein such as 135-ABP, which could achieve the massive and rapid actin disassembly activated during the SI response. Alternatively, unidentified calcium-regulated ABPs may play a role during SI. Future studies will require the identification of new classes of ABPs, careful measurement of cellular concentrations and binding constants for both known and novel ABPs, and detailed examination of the effect of calcium on ABP activity.

Viability of Pollen during Actin Depolymerization

Several pieces of evidence indicate that incompatible pollen is still alive when the major F-actin depolymerization occurs. First, p68 phosphorylation increases at 400 s after SI challenge (Rudd et al., 1997), which coincides with the period of the greatest actin depolymerization. Second, activation of a putative mitogen-activated protein kinase occurs at 5 to 10 min after SI (Rudd and Franklin-Tong, 2002). Furthermore, preliminary data indicate that a putative caspase-like activity is triggered at ~ 30 min in incompatible pollen (N.D. Jordan and V.E. Franklin-Tong, unpublished data). Although we have published pollen viability data previously (Jordan et al., 2000), these were at later time points and therefore are less relevant to this study. Our current data demonstrate that during the period when the dramatic actin depolymerization occurs, the pollen tubes have not lost their viability. Indeed, previous data using differential interference contrast microscopy (Franklin-Tong et al., 1993) indicate that at 6 min after SI challenge, the cytology appears remarkably similar to that in unchallenged pollen tubes except that the clear zone is extended.

How Does Actin Depolymerization Affect Tip Growth?

The key function of SI is to inhibit “self” pollen tube growth. Here, we have demonstrated that F-actin depolymerization is stimulated by the SI response. Because actin depolymerization is not attributable merely to the inhibition of growth, this process plays an active, functional role in the inhibition of tip growth during SI. A crucial difference between pollen grains and tubes is that pollen tubes undergo active tip growth, whereas pollen grains must establish polarity. The delayed SI-induced actin depolymerization response of pollen grains relative to pollen tubes (~ 20 min) corresponds to the time required to determine polarity. This finding indicates that polarity needs to be established before inhibition

and strongly suggests that SI mechanisms act on tip growth. This is consistent with the observation that in incompatible poppy pollen grains, callose is deposited at a single site after polarity has been established.

Tip growth is dependent on a functional actin cytoskeleton (Gibbon et al., 1999; Geitmann and Emons, 2000; Vidali et al., 2001). The population of actin filaments most sensitive to depolymerization is the tip actin, probably because it is the most dynamic (Fu et al., 2001). Analysis of the effects of LatB shows that small amounts of actin depolymerization, or localized depolymerization in the tip region, are sufficient to perturb tip growth (Gibbon et al., 1999). The level of depolymerization observed in the pollen SI response certainly is enough to inhibit tip growth, but it is surprisingly large: at 10 min after SI, it is equivalent to 1000-fold the level required for the inhibition of tip growth by LatB. The sustained depolymerization of the actin cytoskeleton may act as a “fail-safe” mechanism to ensure that tip growth does not resume when $[\text{Ca}^{2+}]_i$ returns to basal levels. Despite the lack of insight regarding the molecular mechanisms involved, this study suggests that Ca^{2+} -mediated actin depolymerization is involved in the inhibition of tip growth.

In summary, our data demonstrate and quantify stimulus-specific actin depolymerization in a plant cell. We propose that tip growth inhibition is achieved, at least in part, through depolymerization of F-actin, and that this is induced via changes in $[\text{Ca}^{2+}]_i$. Surprisingly, the most obvious ABP candidate for this, profilin, does not appear to have sufficient Ca^{2+} -stimulated sequestering activity to account for this depolymerization, at least under the conditions tested. Finally, the sustained nature of the depolymerization is highly unusual and suggests that a programmed cell death signaling pathway may be involved.

METHODS

Pollen Treatments

Pollen from field poppy (*Papaver rhoeas*) was germinated and grown in vitro in liquid germination medium [GM; 0.01% H_3BO_3 , 0.01% KNO_3 , 0.01% $\text{Mg}(\text{NO}_3)_2 \cdot 6\text{H}_2\text{O}$, 0.036% $\text{CaCl}_2 \cdot 2\text{H}_2\text{O}$, and 13.5% Suc] (Jordan et al., 2000). For experiments with pollen grains, pollen was added directly to GM containing recombinant S proteins. For experiments involving the treatment of pollen tubes, pollen grains were sown and left to germinate and grow in GM for a minimum of 60 min (except where stated otherwise), by which time a pollen tube had emerged. S proteins or drugs then were added to these pollen tubes. Recombinant S proteins were produced by cloning the nucleotide sequences specifying the mature peptide of the S_1 and S_3 alleles of the S gene, pPRS100 and pPRS300, respectively, into the expression vector pMS119, as described previously (Foote et al., 1994). Expression and purification of the proteins were as described by Kakeda et al. (1998). The SI response was reproduced in vitro by supplementing GM with recombinant S proteins at a final concentration of 20 $\mu\text{g}/\text{mL}$ for S_1 e and 30 $\mu\text{g}/\text{mL}$ for S_3 e (Geitmann et al.,

2000). Heat-denatured incompatible S proteins (biologically inactive), GM, and solvent at appropriate concentrations were used as controls. Treatments with drugs involved the addition of the appropriate stock to the relevant concentration. Latrunculin B was applied at 100 nM, 1 μ M, or 10 μ M, 4-bromo A-23187 (Calbiochem-Novabiochem Ltd., Nottingham, UK) was applied at 50 μ M, mastoparan was used at 25 μ M, and caffeine (Sigma-Aldrich Co. Ltd., Poole, UK) was applied at 10 mM for the times stated in Results. Controls for these experiments used equivalent amounts of the appropriate solvent for each treatment. Solvents were as follows: for latrunculin B and A-23187, DMSO; for caffeine, GM; for mastoparan, 20 mM Tris, pH 7.5, and 0.5 mM DTT.

Fluorescence Labeling and F-Actin Quantification

Pollen grains and tubes were prepared for F-actin quantification essentially as described by Gibbon et al. (1999). Pollen was stabilized and fixed by the addition of *m*-maleimidobenzoyl-*N*-hydroxysuccinimide ester (Perbio Science UK Ltd., Tattenhall, UK) to a final concentration of 300 μ M. The earliest sampling time point was 1 min, when *m*-maleimidobenzoyl-*N*-hydroxysuccinimide ester was added. Nonidet P-40 was added to a final concentration of 0.05%, and then pollen was collected and washed in GM plus 0.05% Nonidet P-40. Pollen was exchanged into TBSS (50 mM Tris, pH 7.5, 200 mM NaCl, and 400 mM Suc)/0.05% Nonidet P-40 for 1 h, neutralized in TBSS/Nonidet P-40 containing 1 mM DTT, and washed with TBSS/Nonidet P-40. After this cross-linking and extensive washes, pollen was incubated in 2 μ M Alexa-488-phalloidin (Molecular Probes, Eugene, OR) for >2 h, and F-actin levels were determined by eluting bound phalloidin from cells into methanol and subjecting this mixture to spectrophotometry. Fluorescence values were converted to obtain values of phalloidin per pollen grain/tube. Concentrations were derived by dividing these values by the cytoplasmic volume constant of 13 pL for pollen tubes and 8 pL for pollen grains. For pollen grains, the mean diameter (8.0 ± 0.95 μ m; $n = 20$) was used to calculate the volume of a sphere. For pollen tubes, the mean length between the tip and the vacuolar region and the mean width were used to calculate the volume of a cylinder. We assumed that cytoplasmic volume did not change significantly during growth.

Quantification of Total Actin and Total Profilin

Crude pollen extracts from SI-induced pollen grains and tubes were loaded onto 96-well microtiter plates, and the profilin and actin contents were assayed using the ELISA technique used by Gibbon et al. (1999). Native poppy profilin was purified as described (Clarke et al., 1998), and native poppy actin was isolated by DNase I chromatography (Schafer et al., 1998) followed by electroelution from SDS-PAGE gels. Standard curves of purified profilin or actin from poppy pollen were prepared in the range of 0 to 5 ng. Aliquots of 100 ng of protein from pollen tube and grain extracts were added to individual wells, and the amounts of profilin and actin were determined. Polyclonal anti-maize actin serum (Gibbon et al., 1999) was used at a dilution of 1:100, and anti-ZmPRO3 serum (Karakesisoglou et al., 1996) was used at a dilution of 1:1000. Cellular concentrations of profilin and actin were determined using the cytoplasmic volume constants. All statistical analyses between two samples used the two-tailed *t* test. When more than three samples were compared, one-way analysis of variance was performed, as stated in Results.

Protein Estimation

Poppy actin concentrations were determined by scanning densitometry of SDS-PAGE gels using purified maize pollen actin as a standard. Maize pollen actin concentration was determined by measuring absorbance and assuming that an OD₂₉₀ of 0.63 was equal to 1.0 mg/mL (Kovar et al., 2000a). Poppy pollen profilin concentration was determined by measuring absorbance at OD₂₈₀ and using an extinction coefficient of 16,000 M⁻¹·cm⁻¹ (Kovar et al., 2000a). Protein concentrations from total pollen extracts were determined by the Bradford assay (Bio-Rad, Hemel Hempstead, UK) using ovalbumin as a standard.

Measurement of Profilin-Sequestering Activity

The ability of native poppy profilin to bind and prevent the polymerization of pollen actin at steady state was measured by analyzing the shift in critical concentration for actin assembly with 90° light scattering. Apparent *K_d* values were determined when 1 μ M profilin was incubated with varying concentrations of maize pollen actin using the conditions, equations, and assumptions described previously (Kovar et al., 2000a). These assays were repeated at four different calcium concentrations to mimic the conditions in the shank of the pollen tube before and after S protein challenge. Free Ca²⁺ concentration was calculated using CalCalc software (J. Schmid and W. Schreurs, personal communication). The critical concentration values for pollen actin alone were 0.35 ± 0.2 μ M, 0.40 ± 0.08 μ M, 0.39 ± 0.08 μ M, and 0.48 ± 0.04 μ M ($n = 3$ for all) in the presence of 100 nM, 200 nM, 1 μ M, and 2 μ M Ca²⁺, respectively.

Imaging of F-Actin

Samples for cytological analysis were prepared, fixed, and incubated with Alexa-488-phalloidin as described by Gibbon et al. (1999) with the addition of 1% paraformaldehyde to the fixation medium. VECTASHIELD (Vector Labs, Peterborough, UK) was added, and fluorescence microscopy was performed using a Bio-Rad MRC 600 confocal laser scanning microscope equipped with a 25-mW argon-ion laser and a Nikon Diaphot TMD inverted microscope (Nikon UK Ltd., Kingston, UK). A PlanApo $\times 60$ oil-immersion objective, numerical aperture 1.4, and a standard BHS filter block configured for fluorescein isothiocyanate detection were used to collect optical sections through pollen grains and tubes using z-steps spaced 500 nm apart. Image analysis was performed with Confocal Assistant (version 4.02; Bio-Rad), and images were manipulated using Paintshop-Pro (version 5.0; Jase Software, Minneapolis, MN).

Measurement of Pollen Viability during SI

We used fluorescein diacetate (FDA) (Sigma-Aldrich) as a marker for cell viability at a final concentration of 50 μ g/mL. Pollen was grown and challenged with incompatible S proteins on GM, as described previously (Geitmann et al., 2000). At the time intervals indicated in the legend to Figure 5, FDA was added for 5 min. Pollen was imaged using fluorescence microscopy with a fluorescein isothiocyanate filter set. Nonfluorescent FDA is cleaved by active esterases in living cells to generate fluorescein, which accumulates in the cytosol. The number of live pollen grains in several fields of view were counted (~100 to 200 pollen grains), with 3 to 14 independent data sets collected at

0, 10, 20, 40, and 60 min. For each time point, individual percentages were calculated for each data set to obtain the mean percentage of FDA-positive-staining pollen tubes. These data were transformed to angles (arc-sine) for statistical analysis (one-way analysis of variance). Preliminary experiments used propidium iodide (1 $\mu\text{g}/\text{mL}$; incubated for 5 min) to ensure that FDA-positive cells excluded this dye. Mitotracker Red CMXRos (Molecular Probes), which accumulates in functionally active mitochondria, was used at 100 to 200 nM, incubated for 60 min, and viewed using a rhodamine filter set.

Upon request, all novel materials described in this article will be made available in a timely manner for noncommercial research purposes. No restrictions or conditions will be placed on the use of any materials described in this article that would limit their use for non-commercial research purposes.

ACKNOWLEDGMENTS

B.N.S. thanks Bryan Gibbon for advice and training. We are grateful to Mike Kearsley for advice concerning statistical analysis. This work was funded by U.S. Department of Agriculture National Research Initiative Competitive Grants Program (Grant 99-35304-8640) support to C.J.S. and by Biotechnology and Biological Science Research Council (BBSRC) support (to V.E.F.-T.). B.N.S. was funded by a BBSRC committee studentship; we are grateful to the BBSRC for a travel grant. D.R.K. was supported, in part, by a Graduate Assistance in Areas of National Need training grant from the U.S. Department of Education. G.S. is funded by a Royal Society–North Atlantic Treaty Organization Fellowship.

Received March 12, 2002; accepted June 26, 2002.

REFERENCES

- Aizawa, H., Wakatsuki, S., Ishii, A., Moriyama, K., Sasaki, Y., Ohashi, K., Sekine-Aizawa, Y., Sehara-Fujisawa, A., Mizuno, K., Goshima, Y., and Yahara, I. (2001). Phosphorylation of cofilin by LIM-kinase is necessary for semaphorin 3A-induced growth cone collapse. *Nat. Neurosci.* **4**, 367–373.
- Allwood, E.G., Smertenko, A.P., and Hussey, P.J. (2001). Phosphorylation of plant actin-depolymerising factor by calmodulin-like domain protein kinase. *FEBS Lett.* **499**, 97–100.
- Arabidopsis Genome Initiative. (2000). Analysis of the genome sequence of the flowering plant *Arabidopsis thaliana*. *Nature* **408**, 796–815.
- Bamburg, J.R. (1999). Proteins of the ADF/cofilin family: Essential regulators of actin dynamics. *Annu. Rev. Cell Dev. Biol.* **15**, 185–230.
- Becker, K.A., and Hart, N.H. (1999). Reorganization of filamentous actin and myosin-II in zebrafish eggs correlates temporally and spatially with cortical granule exocytosis. *J. Cell Sci.* **112**, 97–110.
- Cárdenas, L., Vidal, L., Domínguez, J., Pérez, H., Sánchez, F., Hepler, P.K., and Quinto, C. (1998). Rearrangement of actin microfilaments in plant root hairs responding to *Rhizobium etli* nodulation signals. *Plant Physiol.* **116**, 871–877.
- Carlsson, L., Markey, F., Blikstad, I., Persson, T., and Lindberg, U. (1979). Reorganization of actin in platelets stimulated by thrombin as measured by DNase I inhibition assay. *Proc. Natl. Acad. Sci. USA* **76**, 6376–6380.
- Clarke, S.R., Staiger, C.J., Gibbon, B.C., and Franklin-Tong, V.E. (1998). A potential signaling role for profilin in pollen of *Papaver rhoeas*. *Plant Cell* **10**, 967–980.
- Cooper, J.A., and Schafer, D.A. (2000). Control of actin assembly and disassembly at filament ends. *Curr. Opin. Cell Biol.* **12**, 97–103.
- del Pozo, O., and Lam, E. (1998). Caspases and programmed cell death in the hypersensitive response of plants to pathogens. *Curr. Biol.* **8**, 1129–1132.
- de Ruijter, N.C.A., Bisseling, T., and Emons, A.M.C. (1999). *Rhizobium* Nod factors induce an increase in sub-apical fine bundles of actin filaments in *Vicia sativa* root hairs within minutes. *Mol. Plant-Microbe Interact.* **12**, 829–832.
- Ding, G., Franki, N., Condeelis, J., and Hays, R.M. (1991). Vasoressin depolymerizes F-actin in toad bladder epithelial cells. *Am. J. Physiol.* **260**, C9–C16.
- Downey, G.P., Chan, C.K., Lea, P., Takai, A., and Grinstein, S. (1992). Phorbol ester-induced actin assembly in neutrophils: Role of protein kinase C. *J. Cell Biol.* **116**, 695–706.
- D'Silva, I., Poirer, G.G., and Heath, M.C. (1998). Activation of cysteine proteases in cowpea plants during the hypersensitive response: A form of programmed cell death. *Exp. Cell Res.* **245**, 389–399.
- Estruch, J.J., Kadwell, S., Merlin, E., and Crossland, L. (1994). Cloning and characterization of a maize pollen-specific calcium-dependent calmodulin-independent protein kinase. *Proc. Natl. Acad. Sci. USA* **91**, 8837–8841.
- Eun, S.-O., and Lee, Y. (1997). Actin filaments of guard cells are reorganized in response to light and abscisic acid. *Plant Physiol.* **115**, 1491–1498.
- Foot, H.C.C., Ride, J.P., Franklin-Tong, V.E., Walker, E.A., Lawrence, M.J., and Franklin, F.C.H. (1994). Cloning and expression of a distinctive class of self-incompatibility (S) gene from *Papaver rhoeas* L. *Proc. Natl. Acad. Sci. USA* **91**, 2265–2269.
- Franklin-Tong, V.E., Dröbak, B.K., Allan, A.C., Watkins, P.A.C., and Trewavas, A.J. (1996). Growth of pollen tubes of *Papaver rhoeas* is regulated by a slow-moving calcium wave propagated by inositol 1,4,5-trisphosphate. *Plant Cell* **8**, 1305–1321.
- Franklin-Tong, V.E., Hackett, G., and Hepler, P.K. (1997). Ratio-imaging of Ca^{2+} in the self-incompatibility response in pollen tubes of *Papaver rhoeas*. *Plant J.* **12**, 1375–1386.
- Franklin-Tong, V.E., Holdaway-Clarke, T.L., Straatman, K.R., Kunkel, J.G., and Hepler, P.K. (2002). Involvement of extracellular calcium influx in the self-incompatibility response of *Papaver rhoeas*. *Plant J.* **29**, 333–345.
- Franklin-Tong, V.E., Ride, J.P., and Franklin, F.C.H. (1995). Recombinant stigmatic self-incompatibility (S-) protein elicits a Ca^{2+} transient in pollen of *Papaver rhoeas*. *Plant J.* **8**, 299–307.
- Franklin-Tong, V.E., Ride, J.P., Read, N.D., Trewavas, A.J., and Franklin, F.C.H. (1993). The self-incompatibility response in *Papaver rhoeas* is mediated by cytosolic free calcium. *Plant J.* **4**, 163–177.
- Fu, Y., Wu, G., and Yang, Z. (2001). Rop GTPase-dependent dynamics of tip-localized F-actin controls tip growth in pollen tubes. *J. Cell Biol.* **152**, 1019–1032.
- Fu, Y., and Yang, Z. (2001). Rop GTPase: A master switch of cell polarity development in plants. *Trends Plant Sci.* **6**, 545–547.
- Geitmann, A., and Emons, A.M.C. (2000). The cytoskeleton in plant and fungal cell tip growth. *J. Microsc.* **198**, 218–245.
- Geitmann, A., Snowman, B.N., Emons, A.M.C., and Franklin-Tong, V.E. (2000). Alterations in the actin cytoskeleton of pollen

- tubes are induced by the self-incompatibility reaction in *Papaver rhoeas*. *Plant Cell* **12**, 1239–1251.
- Gibbon, B.C., Kovar, D.R., and Staiger, C.J.** (1999). Latrunculin B has different effects on pollen germination and tube growth. *Plant Cell* **11**, 2349–2363.
- Gibbon, B.C., and Staiger, C.J.** (2000). Profilin. In *Actin: A Dynamic Framework for Multiple Plant Cell Functions*, C.J. Staiger, F. Baluska, D. Volkmann, and P. Barlow, eds (Dordrecht, The Netherlands: Kluwer Academic Publishers), pp. 45–65.
- Greenberg, S., el Khoury, J., di Virgilio, F., Kaplan, E.M., and Silverstein, S.C.** (1991). Ca^{2+} -independent F-actin assembly and disassembly during Fc receptor-mediated phagocytosis in mouse macrophages. *J. Cell Biol.* **113**, 757–767.
- Gutsche-Perelroizen, I., Lepault, J., Ott, A., and Carlier, M.-F.** (1999). Filament assembly from profilin-actin. *J. Biol. Chem.* **274**, 6234–6243.
- Hall, A.** (1998). Rho GTPases and the actin cytoskeleton. *Science* **279**, 509–514.
- Hall, A.L., Schlein, A., and Condeelis, J.** (1988). Relationship of pseudopod extension to chemotactic hormone-induced actin polymerization in amoeboid cells. *J. Cell. Biochem.* **37**, 285–299.
- Hepler, P.K., Vidali, L., and Cheung, A.Y.** (2001). Polarized cell growth in higher plants. *Annu. Rev. Cell Dev. Biol.* **17**, 159–187.
- Holdaway-Clarke, T.L., Feijó, J.A., Hackett, G.R., Kunkel, J.G., and Hepler, P.K.** (1997). Pollen tube growth and the intracellular cytosolic calcium gradient oscillate in phase while extracellular calcium influx is delayed. *Plant Cell* **9**, 1999–2010.
- Howard, T.H., and Oresajo, C.O.** (1985a). The kinetics of chemotactic peptide-induced change in F-actin content, F-actin distribution, and the shape of neutrophils. *J. Cell Biol.* **101**, 1078–1085.
- Howard, T.H., and Oresajo, C.O.** (1985b). A method for quantifying F-actin in chemotactic peptide activated neutrophils: Study of the effect of tBOC peptide. *Cell Motil.* **5**, 545–557.
- Janmey, P.A.** (1998). The cytoskeleton and cell signaling: Component localization and mechanical coupling. *Physiol. Rev.* **78**, 763–781.
- Jordan, N.D., Franklin, F.C.H., and Franklin-Tong, V.E.** (2000). Evidence for DNA fragmentation triggered in the self-incompatibility response in pollen of *Papaver rhoeas*. *Plant J.* **23**, 471–479.
- Kaiser, D.A., Vinson, V.K., Murphy, D.B., and Pollard, T.D.** (1999). Profilin is predominantly associated with monomeric actin in *Acanthamoeba*. *J. Cell Sci.* **112**, 3779–3790.
- Kakeda, K., Jordan, N.D., Conner, A., Ride, J.P., Franklin-Tong, V.E., and Franklin, F.C.H.** (1998). Identification of residues in a hydrophilic loop of the *Papaver rhoeas* S protein that play a crucial role in recognition of incompatible pollen. *Plant Cell* **10**, 1723–1731.
- Kang, F., Purich, D.L., and Southwick, F.S.** (1999). Profilin promotes barbed-end actin filament assembly without lowering the critical concentration. *J. Biol. Chem.* **274**, 36963–36972.
- Karakesisoglou, I., Schleicher, M., Gibbon, B.C., and Staiger, C.J.** (1996). Plant profilins rescue the aberrant phenotype of profilin-deficient *Dictyostelium* cells. *Cell Motil. Cytoskeleton* **34**, 36–47.
- Karpova, T.S., Tatchell, K., and Cooper, J.A.** (1995). Actin filaments in yeast are unstable in the absence of capping protein or fimbrin. *J. Cell Biol.* **131**, 1483–1493.
- Kobayashi, Y., Kobayashi, I., Funaki, Y., Fujimoto, S., Takemoto, T., and Kunoh, H.** (1997). Dynamic reorganization of microfilaments and microtubules is necessary for the expression of non-host resistance in barley coleoptile cells. *Plant J.* **11**, 525–537.
- Kohno, T., and Shimmen, T.** (1987). Ca^{2+} -induced fragmentation of actin filaments in pollen tubes. *Protoplasma* **141**, 177–179.
- Kohno, T., and Shimmen, T.** (1988). Mechanism of Ca^{2+} inhibition of cytoplasmic streaming in lily pollen tubes. *J. Cell Sci.* **91**, 501–509.
- Korichneva, I., and Hämmerling, U.** (1999). F-actin as a functional target for retro-retinoids: A possible role in anhydroretinol-triggered cell death. *J. Cell Sci.* **112**, 2521–2528.
- Korthout, H.A.A.J., Berecki, G., Bruin, W., van Duijn, B., and Wang, M.** (2000). The presence and subcellular localization of caspase 3-like proteinases in plant cells. *FEBS Lett.* **475**, 139–144.
- Kovar, D.R., Dröbak, B.K., and Staiger, C.J.** (2000a). Maize profilin isoforms are functionally distinct. *Plant Cell* **12**, 583–598.
- Kovar, D.R., and Staiger, C.J.** (2000). Actin depolymerizing factor. In *Actin: A Dynamic Framework for Multiple Plant Cell Functions*, C.J. Staiger, F. Baluska, D. Volkmann, and P. Barlow, eds (Dordrecht, The Netherlands: Kluwer Academic Publishers), pp. 67–85.
- Kovar, D.R., Staiger, C.J., Weaver, E.A., and McCurdy, D.W.** (2000b). AtFim1 is an actin filament crosslinking protein from *Arabidopsis thaliana*. *Plant J.* **24**, 625–636.
- Kreis, T., and Vale, R.** (1999). *Guidebook to the Cytoskeletal and Motor Proteins*, 2nd ed. (New York: Oxford University Press).
- Kurup, S., Ride, J.P., Jordan, N., Fletcher, G., Franklin-Tong, V.E., and Franklin, F.C.H.** (1998). Identification and cloning of related self-incompatibility S-genes in *Papaver rhoeas* and *Papaver nudicaule*. *Sex. Plant Reprod.* **11**, 192–198.
- Lawrence, M.J., Afzal, M., and Kenrick, J.** (1978). The genetical control of self-incompatibility in *Papaver rhoeas* L. *Heredity* **40**, 239–285.
- Levee, M.G., Dabrowska, M.I., Lelli, J.L.J., and Hinshaw, D.B.** (1996). Actin polymerization and depolymerization during apoptosis in HL-60 cells. *Am. J. Physiol.* **271**, C1981–C1992.
- Lillie, S.H., and Brown, S.S.** (1994). Immunofluorescence localization of the unconventional myosin, Myo2p, and the putative kinesin-related protein, Smy1p, to the same regions of polarized growth in *Saccharomyces cerevisiae*. *J. Cell Biol.* **125**, 825–842.
- McCurdy, D.W., Kovar, D.R., and Staiger, C.J.** (2001). Actin and actin-binding proteins in higher plants. *Protoplasma* **215**, 89–104.
- Messerli, M., and Robinson, K.R.** (1997). Tip localized Ca^{2+} pulses are coincident with peak pulsatile growth rates in pollen tubes of *Lilium longiflorum*. *J. Cell Sci.* **110**, 1269–1278.
- Miller, D.D., Callahan, D.A., Gross, D.J., and Hepler, P.K.** (1992). Free Ca^{2+} gradient in growing pollen tubes of *Lilium*. *J. Cell Sci.* **101**, 7–12.
- Miller, D.D., de Ruijter, N.C.A., Bisseling, T., and Emons, A.M.C.** (1999). The role of actin in root hair morphogenesis: Studies with lipochito-oligosaccharide as a growth stimulator and cytochalasin as an actin perturbing drug. *Plant J.* **17**, 141–154.
- Moutinho, A., Hussey, P.J., Trewavas, A.J., and Malhó, R.** (2001). cAMP acts as a second messenger in pollen tube growth and reorientation. *Proc. Natl. Acad. Sci. USA* **98**, 10481–10486.
- Nick, P.** (1999). Signals, motors, morphogenesis: The cytoskeleton in plant development. *Plant Biol.* **1**, 169–179.
- Pierson, E.S., Miller, D.D., Callahan, D.A., van Aken, J., Hackett, G., and Hepler, P.K.** (1996). Tip-localized calcium entry fluctuates during pollen tube growth. *Dev. Biol.* **174**, 160–173.
- Rao, J.Y., Jin, Y.S., Zheng, Q.L., Cheng, J., Tai, J., and Hemstreet, G.P.I.** (1999). Alterations of the actin polymerization status as an apoptotic morphological effector in HL-60 cells. *J. Cell. Biochem.* **75**, 686–697.
- Rathore, K.S., Cork, R.J., and Robinson, K.R.** (1991). A cytoplasmic

- gradient of Ca^{2+} is correlated with the growth of lily pollen tubes. *Dev. Biol.* **148**, 612–619.
- Richael, C., Lincoln, J.E., Bostock, R.M., and Gilchrist, D.G.** (2001). Caspase inhibitors reduce symptom development and limit bacterial proliferation in susceptible plant tissues. *Physiol. Mol. Plant Pathol.* **59**, 213–221.
- Rudd, J.J., Franklin, F.C.H., and Franklin-Tong, V.E.** (1997). Ca^{2+} -independent phosphorylation of a 68 kDa pollen protein is stimulated by the self-incompatibility response in *Papaver rhoeas*. *Plant J.* **12**, 507–514.
- Rudd, J.J., Franklin, F.C.H., Lord, J.M., and Franklin-Tong, V.E.** (1996). Increased phosphorylation of a 26-kD pollen protein is induced by the self-incompatibility response in *Papaver rhoeas*. *Plant Cell* **8**, 713–724.
- Rudd, J.J., and Franklin-Tong, V.E.** (2002). Signals and targets of the self-incompatibility response in pollen of *Papaver rhoeas*. *J. Exp. Bot.*, in press.
- Schafer, D.A., Jennings, P.B., and Cooper, J.A.** (1998). Rapid and efficient purification of actin from nonmuscle sources. *Cell Motil. Cytoskeleton* **39**, 166–171.
- Schlüter, K., Jockusch, B.M., and Rothkegel, M.** (1997). Profilins as regulators of actin dynamics. *Biochim. Biophys. Acta* **1359**, 97–109.
- Schmidt, A., and Hall, M.N.** (1998). Signaling to the actin cytoskeleton. *Annu. Rev. Cell Dev. Biol.* **14**, 305–338.
- Smertenko, A.P., Jiang, C.-J., Simmons, N.J., Weeds, A.G., Davies, D.R., and Hussey, P.J.** (1998). Ser6 in the maize actin-depolymerizing factor, ZmADF3, is phosphorylated by a calcium-stimulated protein kinase and is essential for the control of functional activity. *Plant J.* **14**, 187–194.
- Staiger, C.J.** (2000). Signaling to the actin cytoskeleton in plants. *Annu. Rev. Plant Physiol. Plant Mol. Biol.* **51**, 257–288.
- Staiger, C.J., Baluska, F., Volkmann, D., and Barlow, P.**, eds (2000). *Actin: A Dynamic Framework for Multiple Plant Cell Functions*. (Dordrecht, The Netherlands: Kluwer Academic Publishers).
- Vidali, L., and Hepler, P.K.** (1997). Characterization and localization of profilin in pollen grains and tubes of *Lilium longiflorum*. *Cell Motil. Cytoskeleton* **36**, 323–338.
- Vidali, L., and Hepler, P.K.** (2001). Actin and pollen tube growth. *Protoplasma* **215**, 64–76.
- Vidali, L., McKenna, S.T., and Hepler, P.K.** (2001). Actin polymerization is essential for pollen tube growth. *Mol. Biol. Cell* **12**, 2534–2545.
- Yeh, J., and Haarer, B.K.** (1996). Profilin is required for the normal timing of actin polymerization in response to thermal stress. *FEBS Lett.* **398**, 303–307.
- Yokota, E., Muto, S., and Shimmen, T.** (2000). Calcium-calmodulin suppresses the filamentous actin-binding activity of 135-kilodalton actin-bundling protein isolated from lily pollen tubes. *Plant Physiol.* **123**, 645–654.
- Yokota, E., and Shimmen, T.** (2000). Characterization of native actin-binding proteins from pollen: Myosin and the actin-bundling proteins, 135-ABP and 115-ABP. In *Actin: A Dynamic Framework for Multiple Plant Cell Functions*, C.J. Staiger, F. Baluska, D. Volkmann, and P. Barlow, eds (Dordrecht, The Netherlands: Kluwer Academic Publishers), pp. 103–118.